Ceramics International 47 (2021) 6310–6317

Contents lists available at ScienceDirect

Ceramics International

journal homepage: www.elsevier.com/locate/ceramint

Effect of yttrium-stabilized bismuth bilayer electrolyte thickness on the electrochemical performance of anode-supported solid oxide fuel cells

Dedikarni Panuh [a,b,1], S.A. Muhammed Ali [c,1], Dody Yulianto [b], Muhammad Fadhlullah Shukur [d], Andanastuti Muchtar [a,c,*]

[a] Department of Mechanical and Manufacturing Engineering, Faculty of Engineering and Built Environment, Universiti Kebangsaan Malaysia, 43600, UKM Bangi, Selangor, Malaysia
[b] Department of Mechanical Engineering, Faculty of Engineering, Universitas Islam Riau, Indonesia
[c] Fuel Cell Institute, Universiti Kebangsaan Malaysia, 43600, UKM Bangi, Selangor, Malaysia
[d] Fundamental and Applied Sciences Department, Universiti Teknologi Petronas, 32610, Seri Iskandar, Malaysia

ARTICLE INFO

Keywords:
Bilayer electrolyte
Solid oxide fuel cell
Yttrium stabilized bismuth
Dip-coating

ABSTRACT

Lowering operating temperature and optimizing electrolyte thickness, while maintaining the same high efficiencies are the main considerations in fabricating solid oxide fuel cells (SOFCs). In this study, the effect of yttrium-stabilized bismuth bilayer electrolyte thickness on the electrical performance was investigated. The yttrium-stabilized bismuth bilayer electrolyte was coated on the nickel–samarium-doped composite anode/samarium-doped ceria electrolyte substrate with varying bilayer electrolyte thicknesses (1.5, 3.5, 5.5, and 7.5 μm) via dip-coating technique. Electrochemical performance analysis revealed that the bilayer electrolyte with 5.5 μm thickness exhibited high open circuit voltage, current and power densities of 1.068 V, 259.5 mA/cm^2 and 86 mW/cm^2, respectively at 600 °C. Moreover, electrochemical impedance spectroscopy analysis also exhibited low total polarization resistance (4.64 Ωcm^2) at 600 °C for the single SOFC with 5.5 μm thick yttrium-stabilized bismuth bilayer electrolyte. These findings confirm that the yttrium-stabilized bismuth bilayer electrolyte contributes to oxygen reduction reaction and successfully blocks electronic conduction in $Sm_{0.2}Ce_{0.8}O_{1.9}$ electrolyte materials. This study has successfully produced an $Y_{0.25}Bi_{0.75}O_{1.5}/Sm_{0.2}Ce_{0.8}O_{1.9}$ bilayer system with an extremely low total polarization resistance for low-temperature SOFCs.

1. Introduction

The solid oxide fuel cell (SOFC) is the most promising electrochemical conversion devices for producing electricity from environment-friendly energy sources [1]. SOFCs typically operate at high temperatures between 700 °C and 1000 °C to achieve high efficiency [2]. However, high operating temperatures cause severe thermo–mechanical–chemical instability among components and act as a main barrier for the wide-scale adoption of SOFCs technologies [3,4]. Most studies have focused on the development of intermediate-to low-temperature SOFCs operating at 500 °C-600 °C to expand the application of SOFCs [5,6]. Researchers have mainly focused on the development of new materials or adopted nanostructured architecture and cost-effective processes to achieve highly efficient SOFC technology operating at temperatures between 500 °C and 700 °C [7,8]. However, reducing the operating temperature can induce poor catalytic activity towards oxygen reduction reaction (ORR) rates at the cathode side and diminish ionic conductivity at the electrolyte, which affects the overall electrochemical performance of the SOFC cells [9–12]. The electrocatalytic activity toward the ORR ($O_2 + 4H^+ + 4e^- \rightarrow 2H_2O$) requires four proton-electron transfers to improve its rate-determining process/efficiency at the cathode side, especially at the reduced operating temperature [13,14]. Therefore, high catalytic activity towards ORR and ionic conductivity at the cathode and electrolyte sides are required to increase efficiency at a low-temperature operation, respectively [15]. Typically, lanthanum strontium manganite (LSM) or lanthanum

* Corresponding author. Department of Mechanical and Manufacturing Engineering, Faculty of Engineering and Built Environment, Universiti Kebangsaan Malaysia, 43600, UKM Bangi, Selangor, Malaysia.
E-mail addresses: dedikarni@eng.uir.ac.id (D. Panuh), mas@ukm.edu.my (S.A. Muhammed Ali), dody_yulianto@eng.uir.ac.id (D. Yulianto), mfadhlullah.ashukur@utp.edu.my (M.F. Shukur), muchtar@ukm.edu.my (A. Muchtar).
[1] Equally contributed.

https://doi.org/10.1016/j.ceramint.2020.10.209
Received 9 September 2020; Received in revised form 20 October 2020; Accepted 28 October 2020
Available online 4 November 2020

strontium cobalt ferrite perovskite, yttrium-stabilized zirconia (YSZ), and nickel/YSZ (Ni/YSZ) cermet are the most investigated cathode, electrolyte, and anode materials for high-temperature SOFCs (HT-SOFC), respectively [16].

A conventional YSZ electrolyte material possess high ionic conductivity of 0.1 S/cm at 1000 °C; however its high operating temperature limits its application and also raises the overall cost of the cell [17]. Several studies have been conducted to develop highly conductive solid electrolyte, among which, aliovalent-doped ceria (CeO_2) and isovalent-cation-stabilized bismuth (Bi_2O_3) oxide are especially desirable due to their superior ionic conductivity at low temperatures [1]. For example, bismuth based electrolyte materials such as erbium stabilized bismuth (ESB) [18], yttrium stabilized bismuth (YSB) [19] and co-doped Dy–Gd stabilized bismuth and Dy–Ce stabilized bismuth oxide [20] have been considered promising solid electrolyte materials due to their high conductivity. All these dopants can stabilize bismuth oxide in cubic structures. Among these compositions, YSB exhibits higher ionic conductivity and lower ohmic resistance at the intermediate and low temperatures compared with zirconia-based electrolyte materials [21,22]. Despite high conductivity of YSB, it was not commonly used in SOFCs due to its low thermodynamic stability [23]. This is because Bi_2O_3 electrolyte materials tend decompose to form metallic bismuth at the reducing environment (H_2 and CH_4) [24]. Therefore, YSB electrolyte cannot be used at the electrolyte facing the anode side.

Samarium doped ceria (SDC) or gadolinium-doped ceria (GDC) electrolyte materials has received greater attention for the development of intermediate to low temperature SOFC due to its excellent ionic conductivity and phase stability at low-oxygen partial pressure (PO_2) [25]. However, CeO_2 electrolytes demonstrate mixed ionic-electronic conductive behaviour at low PO_2 ($<10^{-14}$ atm), exhibiting significant n-type electronic conduction through the electrolyte [26]. In addition, the partial reduction of Ce^{4+} to Ce^{3+} contributes to the current leakage, further triggering electronic conduction (>600 °C), resulting in a sudden decline in open circuit voltage (OCV) and low mechanical strength at the reducing environment (anode side) [27,28]. These phenomenon decreases the ionic transference number of the SDC electrolyte; thereby reducing the efficiency of the SOFCs [24]. Therefore, to limit electrical conduction during the application of SOFCs, it is important to enhance the stability and electrolytic domain of these materials. Efforts have focused on blocking electronic conduction by coating a barrier layer on the doped ceria electrolyte side facing the fuel side or the anode side as a means to improve the OCVs and mechanical stability.

The use of bilayer electrolytes is considered to be a simple but effective way of improving the thermodynamic stability of YSB and SDC electrolytes [29]. However, in several of these investigations, zirconia-based YSZ or scandia-stabilized zirconia (ScSZ) electrolyte materials have been used to protect these high conductive materials from decomposition by preventing exposure to reducing environment (anode side) [17,30,31]. This is because zirconia-based electrolytes have demonstrated excellent mechanical and chemical stability in the reducing environment and have also been commonly used as barrier layers for doped ceria electrolyte materials. Heidari et al. [32] reported that the performance of SDC electrolyte-based single SOFCs can be improved using YSZ bilayer electrolyte films and achieve higher OCVs at all operating temperatures. Other electronic current blocking materials were also investigated by researchers for ceria electrolyte [33]. In contrast, our bilayer consists of SDC on the anode side and YSB on the cathode side. This is because the YSB electrolyte layer on the cathode (air) side is expected to obstruct the electronic flow through the SDC layer due to its high transference number (ratio of ionic to total conductivity) [23,34]. The use of SDC and YSB electrolyte materials together often has several benefits, i.e. the presence of SDC layer on the anode side prevents the YSB layer from decomposition in the reducing environment (fuel gases), while the presence of YSB layers blocks electrical leakage through the SDC layer, resulting in high power density and enhanced mechanical stability [35]. A number of studies have demonstrated that OCVs close to 1.0 V can be achieved with ceria/bismuth bilayer as electrolyte at the temperature range of 500–800 °C [36–39]. However, the relative thickness and transport properties of bilayers have a considerable effect on interfacial partial oxygen pressure, which can lead to the electrochemical instability of bilayer electrolyte SOFCs [24]. The decomposition of YSB bilayers can substantially decay the conductivity and increase the ohmic and area-specific resistance of SOFC cells, further resulting in powder density degradation. Optimizing the thickness of the bilayer electrolyte layer is necessary to increase the stability of the SDC electrolytes [40,41]. Mio et al. [40] studied the effect of ESB bilayer thickness on fuel cell performance and found that power density can increase from 84 to 249 mW/cm^2 when the bilayer electrolyte thickness is increased correspondingly from 13 to 20 μm at 500 °C; their study concluded that thin electrolyte layers are highly susceptible to fuel gas erosion.

Advanced deposition techniques based on ceramic powder processing have been used to improve the chemical and physical properties of bilayer electrolyte layers on dense electrolyte substrates [32,42,43]. These methods are well established, but the investment costs for their respective apparatus is higher than that for dip coating [9]. Dip coating is simple, inexpensive and satisfactory method to fabricate thin to thick YSB electrolyte films on SDC electrolytes because the thickness can be easily controlled on the basis of the number of dip coatings [32,44]. In this work, we fabricated the YSB bilayer electrolyte via a simple dip coating process on the uniaxially pressed NiO–SDC/SDC substrate. The present study aims to determine the effect of bilayer thickness (1.5, 3.5, 5.5, and 7.5 μm) on the interfacial polarization resistance and overall performance of bilayer electrolyte cells. An anode-supported single-cell SOFC, with SDC as the electrolyte, YSB as the bilayer electrolyte, Ag–YSB composite as the cathode, and NiO–SDC as the anode, was utilized for this purpose.

2. Experimental procedure

2.1. Powder synthesis and cell fabrication of anode-supported single SOFC

Yttrium oxide (99.999 wt%, Sigma Aldrich Sdn. Bhd), and bismuth (III) oxide (99.999 wt%, Sigma Aldrich Sdn. Bhd) were mixed together in ethanol to prepare YSB bilayer electrolyte via high-speed ball-milling [44]. The SDC ($Ce_{0.8}Sm_{0.2}O_{1.9}$) electrolyte powder was prepared via sol–gel method [45]. All of the reagents were purchased from Sigma Aldrich, Malaysia, with 99.8% purity. Stoichiometric amounts of Sm $(NO_3)_3.6H_2O$ and $Ce(NO_3)_3.6H_2O$ were dissolved together in deionized water and then citric acid (99.8%, Merck Chemicals, Germany) was slowly added to the mixture under continuous stirring. The molar ratio of the total metal ion:citric acid was 1:1.2. The solution mixture was stirred at 80 °C for 12 h to form a viscous gel. The gel was heated continuously to initiate combustion reaction and subsequently a pale yellow colored ash was obtained. The resulting ash was calcined at 850 °C for 5 h to obtain the desired SDC powder. The NiO-SDC composite anode powder was prepared by mixing nickel (II) oxide (99.8%, Sigma Aldrich, Malaysia) with 40 wt% SDC electrolyte powder via high-speed ball milling. Then, the mixed powders were calcined at 1100 °C for 5 h to obtain the NiO–SDC composite anode powder. The slurry for the YSB bilayer electrolyte coating was prepared as follows. First, the YSB electrolyte powder was added to the ethanol (solvent) in a weight ratio of 1:2 and ball-milled for 24 h. Second, α-terpineol (dispersant), polyvinyl butyral (binder), and di-*n*-butyl phthalate (plasticizer) were added to the solvent mixture. Finally, the slurry was ball-milled for 24 h to prepare YSB bilayer electrolyte slurry. The weight ratio between dispersant: binder: plasticizer was 1:3:2. The Ag–YSB, as the cathode ink, was prepared by mixing silver (I) oxide (99.8 wt%, Sigma Aldrich Sdn. Bhd.) and YSB at the weight ratio of 1:1 [44].

The NiO–SDC anode and the SDC electrolyte powders were co-pressed to fabricate NiO-SDC/SDC substrate via a uniaxial pressing

machine. The as-prepared green pellet was co-sintered at 1400 °C for 5 h and used as substrate for depositing the YSB bilayer electrolyte. The NiO–SDC/SDC substrate was dip-coated with YSB slurry and then dried in air for 20 min. The dip-coating and drying were repeated until the desired thickness was achieved. The required dry YSB bilayer electrolyte thickness of ~7.5 μm was achieved after repeating the dip-coating cycle for 5 times. The thickness value ranged from 1 to 1.5 μm after each dipping cycle. The YSB bilayer electrolyte thickness was controlled by maintaining the surface uniformity of the substrate. Finally, the dip-coated YSB bilayer electrolyte film was sintered at 800 °C for 2 h. The effects of thickness on the microstructure and overall performance of the single SOFC was investigated by varying the YSB bilayer thickness from 1.5 to 7.5 μm. The NiO–SDC anode and the SDC/YSB bilayer electrolyte were coated with the Ag–YSB cathode slurry by using the slurry painting method (SPM). The prepared Ag–YSB cathode slurry was deposited on the half-cell and sintered at 800 °C for 2 h. The completed anode-supported single SOFC with different thicknesses of the YSB bilayer electrolyte is presented in Fig. 1.

2.2. Microstructure characterization and electrochemical test of the single SOFC

The thermal decomposition behaviors of the synthesized powders of Ag-YSB, YSB, SDC and NiO-SDC were investigated by thermogravimetry (TG)/differential scanning calorimetry (DSC) (Model 851, Mettler) at the temperature range from 30 °C to 1200 °C with a heating rate of 5 °C/min in air. X-ray diffraction (XRD) patterns were recorded at room temperature using an X-ray diffractometer (Shimadzu XRD-6000) with CuKα (λ = 1.5418 A°) radiation and 2θ ranging from 20° to 80° to identify the crystalline phase of all the synthesized powders. The microstructure of the fabricated anode-supported single SOFC was observed using field emission scanning electron microscopy (FESEM, Zeiss Supra-55 V P, Germany). The elemental distribution of the fabricated anode-supported single SOFC was determined through energy-dispersive X-ray spectroscopy (EDS). The effect of YSB electrolyte thickness on the electrochemical performance of the fabricated single SOFCs was tested using a solid oxide fuel cell testing machine (CHINO, Japan) from 500 °C to 600 °C using hydrogen (60 mL/min) and air (100 mL/min) as the fuel and oxidant, respectively. The effective working area of the pellet was 0.8 cm^2. The current (I)-voltage (V) and power density (P) curves were measured with a Multi-channel Potentiostat/Galvanostat (Autolab AUT302 FRA). The electrochemical impedance spectra (EIS) were collected by a frequency response analyzer (FRA) (Autolab 302, Eco Chemie, Netherlands) under open circuit voltage condition over a frequency range of 10^6 Hz–0.1 Hz with a 10 mV amplitude to determine the effect of YSB bilayer thickness on the single SOFC performance. The ohmic résistance (R_0) and total interfacial polarization resistance (R_P) were determined from the impedance spectra.

3. Results and discussion

3.1. TGA/DSC analysis

The TGA/DSC analysis was conducted to examine the thermal behaviour of all the synthesized powders of Ag-YSB, YSB, SDC and NiO-SDC between 30 °C and 1200 °C, as shown in Fig. 2. No significant weight loss from the synthesized powders of NiO-SDC composite anode, SDC electrolyte and YSB bilayer electrolyte powders were observed from the TGA curve. This can be attributed to the no use of any organic and polymeric agents during the synthesis process. However, the highest weight loss was observed for the Ag-YSB cathode powders. The TGA curve showed a ~7% weight loss between 330 °C and 1000 °C for the Ag-YSB cathode powder. In the same temperature range, the DTA curve showed an endothermic peak positioned at ~950 °C, which is associated to the melting and decomposition behaviour of Ag_2O_3 in the Ag-YSB composite cathode powder. However, this decomposition behaviour of Ag_2O_3 was not observed between the actual SOFC operating temperature range between 500 and 600 °C and exhibited only ~3% weight loss between this temperature. Thus, indicating an absence of decomposition or volatilization of Ag_2O_3 during the SOFC operation and sintering temperature. Two exothermic peaks were observed from the DTA curve at ~180 °C and ~340 °C for all the synthesized powders, indicating the occurrence of glass transition phase and crystallization, respectively. This crystallization peaks at ~340 °C confirms that the crystallization

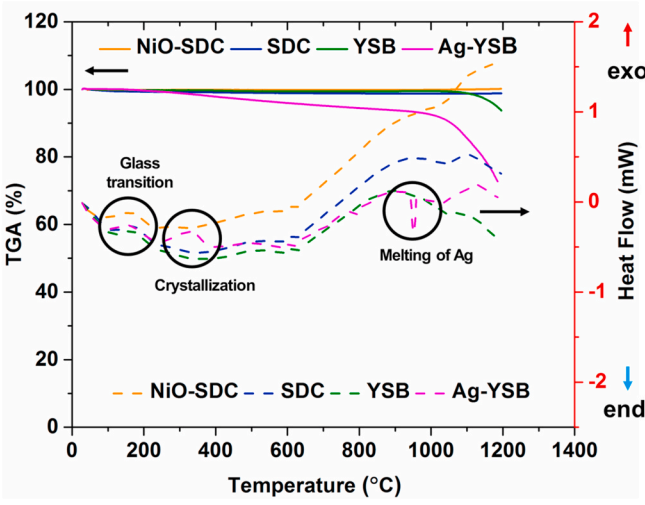

Fig. 2. TGA and DSC curve of NiO-SDC anode, SDC electrolyte, YSB bilayer electrolyte and Ag-YSB cathode powders.

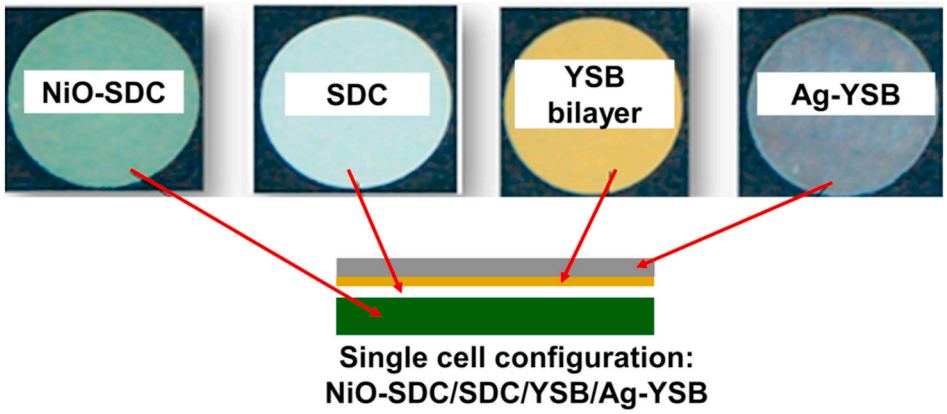

Fig. 1. Schematic configuration of NiO-SDC/SDC/YSB/Ag-YSB as a single SOFC.

occurs in the samples. These TGA and DTA data were used to determine the crystallization temperature for the synthesized powders.

3.2. XRD analysis

X-ray diffraction patterns were used to determine the phase formation and degree of crystallinity of all the synthesized powders, as shown in Fig. 3 (a)-(d). Table 1 shows the composition, phase structure, calcination temperature and crystallite size of all the synthesized powders. The phase analysis data of NiO-SDC composite anode and SDC powders confirmed that no phase changes or any chemical reaction occurred between NiO and SDC during synthesis and calcination, as shown in Fig. 3(a–b). No additional or secondary peaks as impurities were observed for the prepared composite anode powders, thereby demonstrating excellent chemical compatibility after mixing and calcination. The two main phase structures of single-crystalline cubic NiO and face-centered cubic fluorite SDC were identified. However, the crystallite size of the SDC electrolyte increased after mixing and calcination with NiO powder (Table 1). This is due to the higher calcination temperature used to prepare NiO-SDC composite anode powder (1100 °C/5 h). Fig. 3(c–d) show the XRD pattern of the YSB bilayer electrolyte and Ag-YSB composite cathode powders. The pure cubic YSB phase and main peaks of metallic Ag is evident from the XRD pattern, as shown in Fig. 3(d). A large amount of metallic Ag is detected due to low calcination temperature (600 °C/2 h) [46]. However, few Ag_2O_3 peaks were also detected. It is evident from the XRD pattern that the YSB peak shifted to lower theta angle after addition of Ag_2O_3. This peak shift can be attributed to the higher ionic radii of the six coordinated Ag^{2+} ion (0.94 Å) and could have induced the expansion of Bi_2O_3 phase [47]. The crystallite sizes of the synthesized powders were determined by the Debye-Scherrer formula ($D = 0.9\lambda/(\beta - b)\cos\theta$), where D is the crystallite size, λ is the wavelength of the X-ray radiation, β is the full width at half maximum of intensity of the diffraction peak, b is standard instrumental broadening (0.0578°) and θ is the Bragg diffraction angle of peak.

3.3. Microstructure of the single SOFC

The cross-sectional FESEM micrographs of NiO-SDC/SDC anode supported single SOFC with 7.5 μm thick YSB bilayer electrolyte at two different magnifications are shown in Fig. 4(a–b). The anode-supported single SOFC with 1000 μm NiO-SDC composite anode, 500 μm SDC/YSB bilayer and 50 μm Ag-YSB composite is clearly distinguishable and no cracks were visible between the layers (Fig. 4 (a)). At higher magnification (Fig. 4 (b)), finer microstructure of YSB bilayer electrolyte can be distinguished between the SDC electrolyte and Ag-YSB composite cathode layers. The YSB bilayer electrolyte thickness was varied between 1.5 μm–7.5 μm and the layer appears to be porous with asymmetric grains, as shown in Fig. 5(a–b). On the other hand, the microstructure of SDC electrolyte appears to be quite dense with some closed pores. To determine for any obvious interdiffusion of constituent elements between the fabricated layers, the compositional analysis at the anode and cathode layers were conducted with the EDS technique, as shown in Fig. 4(c–d). Ni, Ce, Sm is only present in the NiO-SDC composite anode layer (Fig. 4(d)). Similarly, elements such as Ag, Bi and Y are only observed in the Ag-YSB composite cathode layer. This clearly indicates that no obvious interdiffusion of elements between the Ag-YSB and NiO-SDC layers through SDC/YSB layers was observed. This assures the stability of the layers during the fabrication and sintering processes.

As shown by the cross-sectional images in Fig. 5(a)–(b), the bilayer electrolyte YSB particles are homogenously distributed along the SDC electrolyte substrate. The YSB bilayer appeared to be porous and adhered well to the SDC electrolyte and Ag-YSB composite cathode with no delamination or cracks. The YSB bilayer thickness increased gradually from 1.5 to 7.5 μm as the number of layers increased.

Table 1
Composition, phase structure, calcination temperature and crystallite size of the synthesized powders.

Components	Composition	Phase structure	Calcination temperature (°C)/time (hours)	Crystallite size (nm)
Electrolyte	$Sm_{0.2}Ce_{0.8}O_{1.9}$ (SDC)	Cubic	850/5	42
Bilayer	$Y_{0.25}Bi_{0.75}O_{1.5}$ (YSB)	Cubic	750/2	29
Anode	60 wt% NiO-40% SDC	Cubic	1100/5	116 (NiO) & 80 (SDC)
Cathode	50 wt% Ag-50% YSB	Cubic	600/2	29

3.4. Single SOFC electrochemical performance

The electrochemical performance of the fabricated NiO-SDC/SDC anode-supported single SOFC with different YSB bilayer electrolyte thicknesses (1.5, 3.5, 5.5, and 7.5 μm) was investigated at 500 °C-600 °C in air and hydrogen. *I–V* and *I–P* characteristics of the fabricated anode supported cell with different YSB bilayer electrolyte measured at 600 °C are shown in Fig. 6. It is evident that the electrochemical performance of the fabricated anode-supported single SOFC increased as the thickness of the YSB bilayer electrolyte increased. The maximum OCV of the anode-

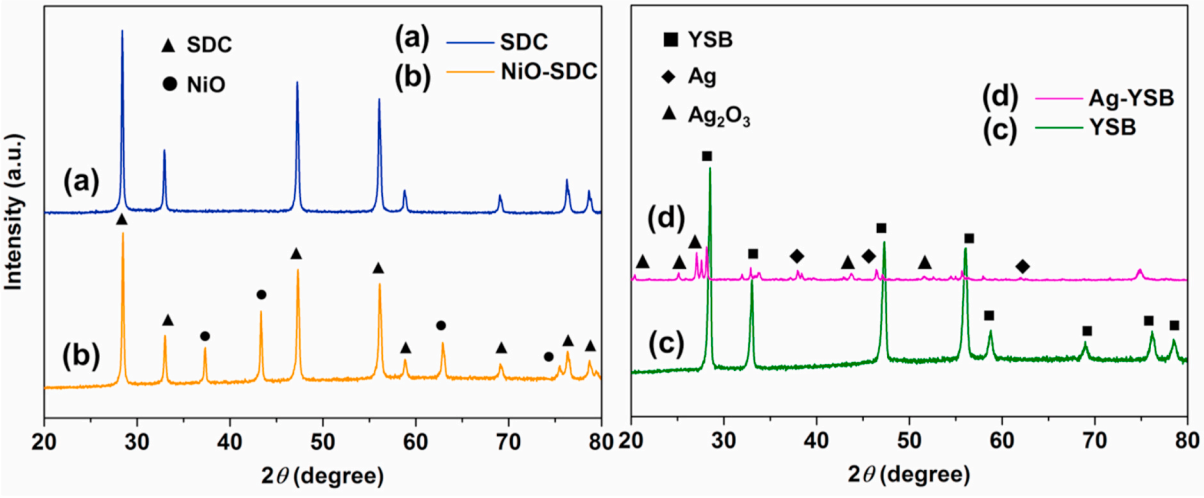

Fig. 3. XRD patterns of (a) NiO-SDC composite anode, (b) SDC electrolyte, (c) YSB bilayer electrolyte, (d) Ag-YSB cathode powders.

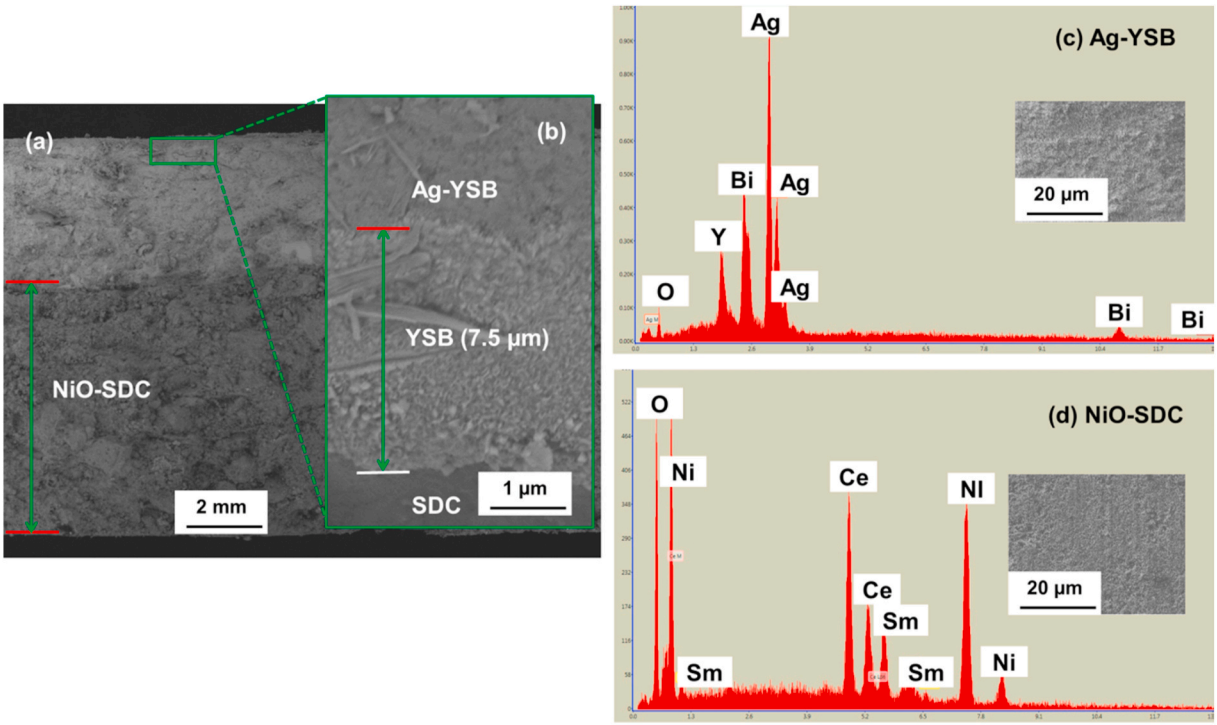

Fig. 4. Cross-sectional FESEM images of NiO-SDC/SDC/YSB/Ag-YSB single SOFC at two different magnification: (a) 80× and (b) 10,000 ×; EDS elemental analysis of: (c) Ag-YSB composite cathode, and (d) NiO-SDC composite anode.

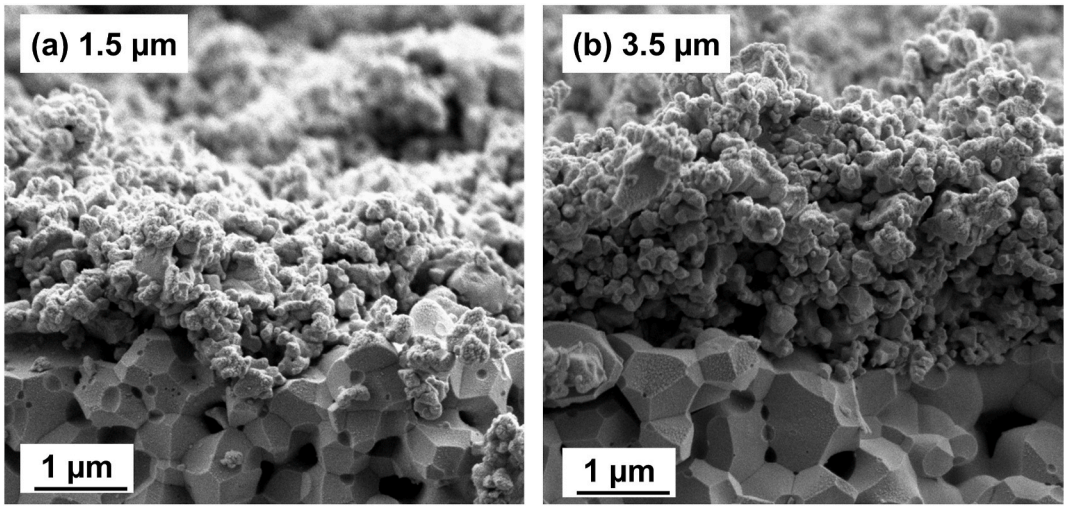

Fig. 5. FESEM image of the YSB bilayer electrolytes with different thicknesses (a) 1.5, and (b) 3.5 μm.

supported single SOFC with different thicknesses of 1.5, 3.5, 5.5 and 7.5 μm reached 0.99 V, 1.074 V, 1.068 V, and 1.072 V, respectively at an operating temperature of 600 °C. Moreover, it is noteworthy that the OCVs of all the fabricated single SOFCs were extremely close to the theoretical values, due to the highly dense SDC electrolyte as observed in Fig. 4(b) [36]. The maximum power densities of the NiO-SDC/SDC anode supported cells at 600 °C with YSB bilayer thicknesses of 1.5, 3.5, 5.5 and 7.5 μm were 26.3, 61.5, 86, and 79.2 mW/cm^2, respectively. As shown in Fig. 6, the single SOFC with 5.5 μm-thick YSB bilayer electrolytes exhibited a maximum power density of 86 mW/cm^2 and a current density of 259.5 mA/cm^2 at 600 °C. All of the anode-supported single SOFCs in this study were manufactured in a similar way but exhibited different OCVs and power densities due to the variations in thickness of the YSB bilayer electrolyte. Jaiswal et al. [37] also reported a similar finding for bismuth-based bilayer electrolyte materials with relatively high thicknesses. This indicates that electrochemical, performance of the NiO-SDC/SDC anode supported single SOFC can be increased by forming a pure oxide-ion conducting and electron-blocking functional layer [40]. Moreover, the presence of thick SDC layer is beneficial to YSB electrolyte stability. The YSB bilayer electrolyte materials in this study yielded higher OCV results than those in previous research. For instance, Zhang et al. [19] investigated a single cell with NiO/SDC/SDC/YSB/LSM-YSM configuration and reported the maximum OCV value of 0.897 V at 600 °C. From Fig. 7 (a)-(c), it is evident that the maximum power density increased from 14.8 mW/cm^2 to 86 mW/cm^2 as the operating temperature increased from 500 to 600 °C. This is due to increased ionic conductivity of the electrolyte and faster electrode catalytic activity with the increasing temperature [48].

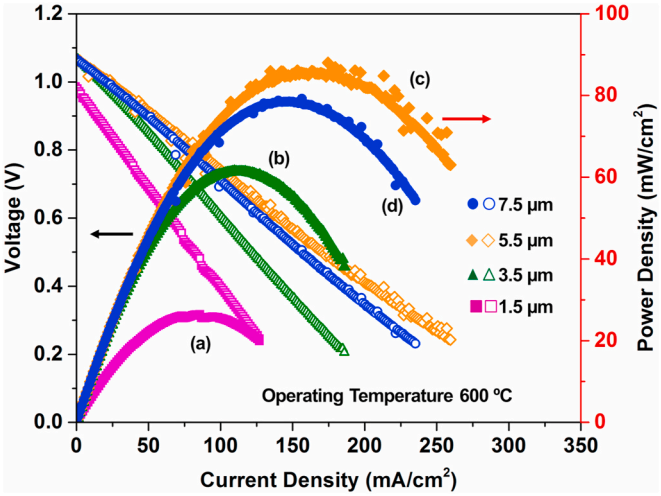

Fig. 6. Electrochemical performance of single SOFC with different YSB bilayer thicknesses at 600 °C: (a) 1.5 μm, (b) 3.5 μm, (c) 5.5 μm, and (d) 7.5 μm.

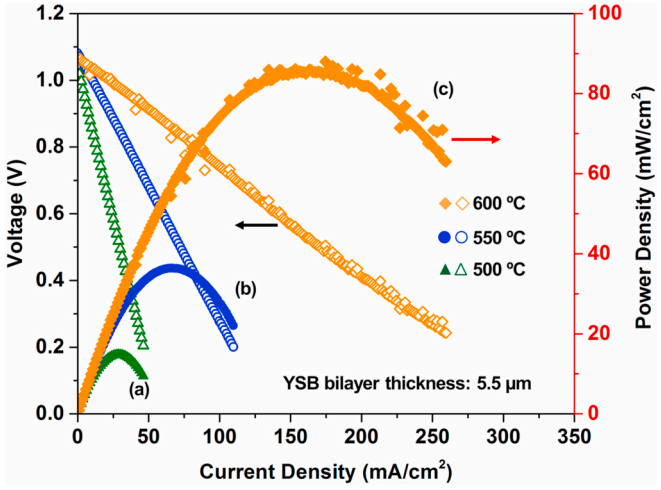

Fig. 7. Electrochemical performance of a single SOFC with 5.5 μm thick YSB bilayer thicknesses at: (a) 500 °C, (b) 550 °C, and (c) 600 °C.

The effect of the thickness variation of the YSB bilayer electrolyte on the performance difference needs to be further explored. Thus, the EIS technique was employed on the single SOFCs at 600 °C under OCV. Fig. 8 shows the corresponding impedance spectra measured at 600 °C for the NiO-SDC/SDC anode supported cell with different YSB bilayer electrolytes. The following equivalent circuit (insert) was used to investigate the electrical behaviour at 600 °C, where R_{ele} is the ohmic resistance from the electrolyte (first semicircle at high frequency), R_{cath} is attributed to the charge transfer resistance from the cathode (second semicircle at middle frequency), R_{ano} is attributed to the gas diffusion resistance at the anode (third semicircle at low frequency), and CPE is the constant phase element. All the samples exhibited three arcs in the complex impedance plane featuring the frequency-dependent semicircles related to the electrolyte (R_{ele}) cathode (R_{cath}) and anode (R_{ano}) responses, respectively. The ohmic resistance of the electrolyte/bilayer electrolyte decreased as the YSB bilayer electrolyte thickness increased to 5.5 μm and began to increase again when YSB bilayer electrolyte is > 5.5 μm. The ohmic resistance was found to be 4.95 Ωcm^2, 3.27 Ωcm^2, 3.1 Ωcm^{2}and 3.21 Ωcm^2 for the single SOFC with 1.5, 3.5, 5.5, and 7.5 μm-thick YSB bilayer electrolytes, respectively. Moreover, the total polarization resistance (R_{tot}) of the anode-supported cell also decreased as the YSB bilayer thickness increased. The R_{tot} of the anode-supported single

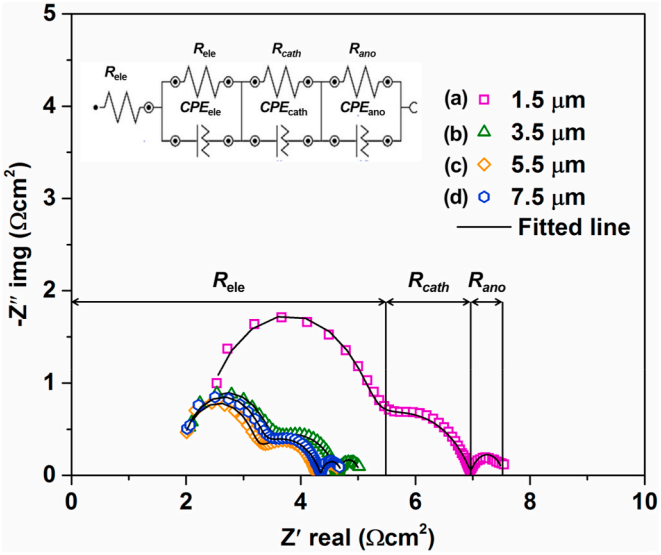

Fig. 8. Impedance spectra of the anode-supported single SOFC with different YSB bilayer thicknesses at 600 °C: (a) 1.5 μm, (b) 3.5 μm, (c) 5.5 μm, and (d) 7.5 μm.

SOFC was calculated using the sum of both ohmic resistance and interfacial polarization resistance from the electrolyte and electrodes, respectively. The total resistance was found to be 7.53 Ωcm^2, 5.03 Ωcm^2, 4.64 Ωcm^2 and 4.73 Ωcm^2 for the fabricated single SOFCs with 1.5, 3.5, 5.5, and 7.5 μm-thick YSB bilayer electrolytes, respectively. This decrease in total polarization resistance was greatly influenced by the interfacial polarization resistance ($R_P = R_{cath} + R_{ano}$) from the electrodes, especially from the cathode side.

The cathodic polarization resistance (R_{cath}) from the Ag-YSB cathode decreased as the YSB bilayer thickness increased from 1.5 μm to 7.5 μm as shown in Fig. 8. The R_{cath} value was found to be 2.53 Ωcm^2, 1.73 Ωcm^2, 1.48 Ωcm^2 and 1.43 Ωcm^2 for the single SOFC with 1.5, 3.5, 5.5, and 7.5 μm-thick YSB bilayer electrolytes, respectively. Because of the high conductivity of the YSB electrolyte, it is apparent that the ohmic resistance of the anode-supported single SOFC did not demonstrate a noticeable change due to the increase in the thickness of the YSB bilayer electrolyte. However, the R_P of the anode-supported single SOFC with 5.5 μm thickness was much lower than that of the single SOFC with 1.5 μm-thick YSB bilayer electrolyte due to the positive effect of the YSB bilayer on cathodic polarization. This decrease in R_{cath} can be attributed to the increased thickness of the YSB bilayer electrolyte. The explanation for this is that the YSB bilayer electrolyte demonstrates a pure ion-conducting oxide behaviour that enhanced the oxygen dissociation and surface oxygen exchange rate [33,49]. This is because the bilayered electrolyte can be used as both an electronic conduction barrier and an oxygen–ion-conducting phase in the cathode structure, thus, the YSB bilayer electrolyte, as a pure oxide ion conductor, manifested positive effect [21]. It should be noted that the increase in maximum powder density for single SOFC with 5.5 μm-thick YSB electrolyte is a function of the operating temperature and YSB bilayer thickness. Therefore, an improvement in the thickness of the YSB bilayer electrolyte contributes to an increase in the length of the ion transfer pathway in the electrolyte, which leads to an increase in the power density. The sample with the 5.5 μm-thick YSB bilayer electrolyte exhibited low total resistance (4.64 Ωcm^2) at 600 °C. However, the performance obtained from this study was lower or simply comparable with the reported values for several bismuth bilayer electrolyte-based fuel cells (Table 2). The differences in performance between the present and previous studies can be explained by the variation in materials and bilayer electrolyte thickness. Therefore, the optimization of material compositions, fabrication parameters, and electrolyte and bilayer electrolyte thickness could contribute to the

Table 2
Comparison of single-cell performance of bismuth bilayer electrolyte materials.

Single SOFC configuration: Anode/ Electrolyte/ Bilayer/Cathode	Bilayer thickness (μm)	Operating temperature (°C)	Power density (mW/cm^2)	Reference
NiO-SDC/SDC/ YSB/Ag-YSB	5.5	600	86	This study
NiO-GDC/GDC/ xSB/LSM-ESB	20.6	650	1060	[37]
NiCuO-SNDC/ SNDC/ESB/ LSM-ESB	20	450	129	[40]
NiO-BCZY/BCZY/ BCY/SSC-SDC	3.6	700	163	[42]
Pt/SDC/Au	–	800	40	[50]
NiO-YSZ/YSZ/ ESB/LSM-ESB	5.1	700	2100	[51]

increase in the OCV value and overall performance of the fuel cell.

4. Conclusion

The dip-coating technique was used in this study to coat the YSB electronic blocking functional layer on the NiO–SDC/SDC substrate. The YSB layer thickness was varied from 1.5 to 7.5 μm. The OCV values were 0.99 V, 1.074 V, 1.068 V, and 1.072 V, while the respective YSB layer thicknesses were 1.5, 3.5, 5.5 and 7.5 at 600 °C. The result indicates that thick YSB layers can block the electronic conduction in SDC electrolytes and increased the OCV values compared with cells with <5.5 μm thickness. The single SOFC with 5.5 μm-thick YSB bilayer electrolytes exhibited a maximum power density of 86 mW/cm^2 and a current density of 259.5 mA/cm^2 at 600 °C. However, the power densities of the cells obtained from this study are not high enough for low-to intermediate-temperature SOFC operation. Thus, further improvement is needed to expand the ionic conductivity of bilayer electrolytes.

Declaration of competing interest

The authors declare that they have no known competing financial interests or personal relationships that could have appeared to influence the work reported in this paper.

Acknowledgments

This work was supported by Universiti Kebangsaan Malaysia (UKM), Universiti Teknologi Petronas, and Universitas Islam Riau under the research sponsorships of MI/2019/019, 468/Kontrak/LPM-UIR-9-2018, and 361/Kontrak/LPPM-UIR/4–2018, respectively. The authors would also like to acknowledge the support of the Centre for Research and Instrumentation Management, UKM, for the testing equipment.

References

[1] R. Raza, B. Zhu, A. Rafique, M.R. Naqvi, P. Lund, Functional ceria-based nanocomposites for advanced low-temperature (300–600 °C) solid oxide fuel cell: a comprehensive review, Mater. Today Energy. 15 (2020), 100373.
[2] A.M. Hussain, K.-J. Pan, I.A. Robinson, T. Hays, E.D. Wachsman, Stannate-based ceramic oxide as anode materials for oxide-ion conducting low-temperature solid oxide fuel cells, J. Electrochem. Soc. 163 (2016) F1198–F1205.
[3] C. Zhou, J. Sunarso, Y. Song, J. Dai, J. Zhang, B. Gu, W. Zhou, Z. Shao, New reduced-temperature ceramic fuel cells with dual-ion conducting electrolyte and triple-conducting double perovskite cathode, J. Mater. Chem. A. 7 (2019) 13265–13274.
[4] T.B. Mitchell-Williams, R.I. Tomov, S.A. Saadabadi, M. Krauz, P.V. Aravind, B. A. Glowacki, R.V. Kumar, Infiltration of commercially available, anode supported SOFC's via inkjet printing, Mater. Renew. Sustain. Energy. 6 (2017) 12.
[5] Y.L. Huang, A.M. Hussain, E.D. Wachsman, Nanoscale cathode modification for high performance and stable low-temperature solid oxide fuel cells (SOFCs), Nanomater. Energy 49 (2018) 186–192.
[6] S.P.S. Shaikh, A. Muchtar, M.R. Somalu, A review on the selection of anode materials for solid-oxide fuel cells, Renew. Sustain. Energy Rev. 51 (2015) 1–8.
[7] M. Anwar, M.A. Muhammed, A. Muchtar, M.R. Somalu, Influence of strontium co-doping on the structural, optical, and electrical properties of erbium-doped ceria electrolyte for intermediate temperature solid oxide fuel cells, Ceram. Int. 45 (2019) 5627–5636.
[8] S.A. Muhammed Ali, M. Anwar, L.S. Mahmud, N.S. Kalib, A. Muchtar, M. R. Somalu, Influence of current collecting and functional layer thickness on the performance stability of La0.6Sr0.4Co0.2Fe0.8O3-δ -Ce0.8Sm0.2O1.9 composite cathode, J. Solid State Electrochem. 23 (2019) 1155–1164.
[9] N. Hedayat, D. Panthi, Y. Du, Fabrication of anode-supported microtubular solid oxide fuel cells by sequential dip-coating and reduced sintering steps, Electrochim. Acta 258 (2017) 694–702.
[10] Y.C. Yang, P.H. Wang, Y.T. Tsai, H.C. Ong, Influences of feedstock and plasma spraying parameters on the fabrication of tubular solid oxide fuel cell anodes, Ceram. Int. 44 (2018) 7824–7830.
[11] T. Pirasaci, Non-uniform, multi-stack solid oxide fuel cell (SOFC) system design for small system size and high efficiency, J. Power Sources 426 (2019) 135–142.
[12] A.M. Soydan, Ö. Yıldız, A. Durğun, O.Y. Akduman, A. Ata, Production, performance and cost analysis of anode-supported NiO-YSZ micro-tubular SOFCs, Int. J. Hydrogen Energy 44 (2019) 30339–30347.
[13] A.D. Handoko, S.N. Steinmann, Z.W. Seh, Theory-guided materials design: two-dimensional MXenes in electro- and photocatalysis, Nanoscale Horizons 4 (2019) 809–827.
[14] Z.W. Seh, J. Kibsgaard, C.F. Dickens, I. Chorkendorff, J.K. Nørskov, T.F. Jaramillo, Combining theory and experiment in electrocatalysis: insights into materials design, Science 84 355 (2017) 4998.
[15] Y. Lyu, J. Xie, D. Wang, J. Wang, Review of cell performance in solid oxide fuel cells, J. Mater. Sci. 55 (2020) 7184–7207.
[16] S.P. Jiang, Development of lanthanum strontium cobalt ferrite perovskite electrodes of solid oxide fuel cells – a review, Int. J. Hydrogen Energy 44 (2019) 7448–7493.
[17] S. Cho, Y. Kim, J.H. Kim, A. Manthiram, H. Wang, High power density thin film SOFCs with YSZ/GDC bilayer electrolyte, Electrochim. Acta 56 (2011) 5472–5477.
[18] J.S. Ahn, M.A. Camaratta, D. Pergolesi, K.T. Lee, H. Yoon, B.W. Lee, D.W. Jung, E. Traversa, E.D. Wachsman, Development of high performance ceria/bismuth oxide bilayered electrolyte SOFCs for lower temperature operation, J. Electrochem. Soc. 157 (2010) B376.
[19] L. Zhang, C. Xia, F. Zhao, F. Chen, Thin film ceria-bismuth bilayer electrolytes for intermediate temperature solid oxide fuel cells with La0.85Sr0.15MnO3-δ-Y0.25Bi0.75O1.5 cathodes, Mater. Res. Bull. 45 (2010) 603–608.
[20] A.L. Ruth, K.T. Lee, M. Clites, E.D. Wachsman, Synthesis and characterization of double-doped bismuth oxide electrolytes for lower temperature SOFC application, ECS Trans 64 (2014) 135–141.
[21] G. Li, B. He, Y. Ling, J. Xu, L. Zhao, Highly active YSB infiltrated LSCF cathode for proton conducting solid oxide fuel cells, Int. J. Hydrogen Energy 40 (2015) 13576–13582.
[22] H. Ozlu Torun, S. Cakar, E. Ersoy, O. Turkoglu, The bulk electrical conductivity properties of δ-Bi2O3 solid electrolyte system doped with Yb2O3, J. Therm. Anal. Calorim. 122 (2015) 525–536.
[23] E.D. Wachsman, K.T. Lee, Lowering the temperature of solid oxide fuel cells, Science 334 (80) (2011) 935–939.
[24] J.Y. Park, E.D. Wachsman, Stable and high conductivity ceria/bismuth oxide bilayer electrolytes for lower temperature solid oxide fuel cells, Ionics 12 (2006) 15–20.
[25] M. Biswas, K. Sadanala, Electrolyte materials for solid oxide fuel cells (SOFCs), Powder Metall. Min. 2 (2013) 26–55.
[26] M. Liu, F. Uba, Y. Liu, A high-performance solid oxide fuel cell with a layered electrolyte for reduced temperatures, J. Am. Ceram. Soc. 103 (2020) 5325–5336.
[27] M. Anwar, S.A. Muhammed Ali, A. Muchtar, M.R. Somalu, Synthesis and characterization of M-doped ceria-ternary carbonate composite electrolytes (M = erbium, lanthanum and strontium) for low-temperature solid oxide fuel cells, J. Alloys Compd. 775 (2019) 571–580.
[28] Y.D. Kim, J. Yang, J.I. Lee, M. Saqib, J.S. Shin, K. Park, M. Jo, S.J. Song, J.Y. Park, Degradation studies of ceria-based solid oxide fuel cells at intermediate temperature under various load conditions, J. Power Sources 452 (2020) 227758.
[29] J. Kim, J. Kim, K.J. Yoon, J.-W. Son, J.-H. Lee, J.-H. Lee, H.-W. Lee, H.-I. Ji, Solid oxide fuel cells with zirconia/ceria bilayer electrolytes via roll calendering process, J. Alloys Compd. 846 (2020) 156318.
[30] C. Kim, S. Kim, I. Jang, H. Yoon, T. Song, U. Paik, Facile fabrication strategy of highly dense gadolinium-doped ceria/yttria-stabilized zirconia bilayer electrolyte via cold isostatic pressing for low temperature solid oxide fuel cells, J. Power Sources 415 (2019) 112–118.
[31] P. Coddet, M.L. Amany, J. Vulliet, A. Caillard, A.L. Thomann, YSZ/GDC bilayer and gradient barrier layers deposited by reactive magnetron sputtering for solid oxide cells, Surf. Coating. Technol. 357 (2019) 103–113.
[32] D. Heidari, S. Javadpour, S.H. Chan, An evaluation of electrochemical performance of a solid oxide electrolyzer cell as a function of co-sintered YSZ-SDC bilayer electrolyte thickness, Energy Convers. Manag. 150 (2017) 567–573.
[33] J.S. Ahn, D. Pergolesi, M.A. Camaratta, H. Yoon, B.W. Lee, K.T. Lee, D.W. Jung, E. Traversa, E.D. Wachsman, High-performance bilayered electrolyte intermediate temperature solid oxide fuel cells, Electrochem, Commun. Now. 11 (2009) 1504–1507.
[34] N. Jiang, E.D. Wachsman, S.H. Jung, A higher conductivity Bi2O3-based electrolyte, Solid State Ionics 150 (2002) 347–353.

[35] K.T. Lee, D.W. Jung, M.A. Camaratta, H.S. Yoon, J.S. Ahn, E.D. Wachsman, Gd0.1Ce0.9O1.95/Er0.4Bi1.6O3 bilayered electrolytes fabricated by a simple colloidal route using nano-sized Er0.4Bi1.6O3 powders for high performance low temperature solid oxide fuel cells, J. Power Sources 205 (2012) 122–128.
[36] D.W. Joh, J.H. Park, D. Kim, E.D. Wachsman, K.T. Lee, Functionally graded bismuth oxide/zirconia bilayer electrolytes for high-performance intermediate-temperature solid oxide fuel cells (IT-SOFCs), ACS Appl. Mater. Interfaces 9 (2017) 8443–8449.
[37] A. Jaiswal, A. Pesaran, S. Omar, E.D. Wachsman, Ceria/bismuth oxide bilayer electrolyte based low-temperature SOFCs with stable electrochemical performance, ECS Trans 78 (2017) 361–370.
[38] J. Hou, L. Bi, J. Qian, Z. Zhu, J. Zhang, W. Liu, High performance ceria-bismuth bilayer electrolyte low temperature solid oxide fuel cells (LT-SOFCs) fabricated by combining co-pressing with drop-coating, J. Mater. Chem. A. 3 (2015) 10219–10224.
[39] A. Pesaran, A. Jaiswal, Y. Ren, E.D. Wachsman, Development of a new ceria/yttria-ceria double-doped bismuth oxide bilayer electrolyte low-temperature SOFC with higher stability, Ionics 25 (2019) 3153–3164.
[40] L. Miao, J. Hou, K. Dong, W. Liu, A strategy for improving the sinterability and electrochemical properties of ceria-based LT-SOFCs using bismuth oxide additive, Int. J. Hydrogen Energy 44 (2019) 5447–5453.
[41] Y.D. Kim, J.Y. Yang, J.I. Lee, M. Saqib, J.S. Shin, M. Shin, J.H. Kim, H.T. Lim, J. Y. Park, Stable ceria-based electrolytes for intermediate temperature-solid oxide fuel cells via hafnium oxide blocking layer, J. Alloys Compd. 779 (2019) 121–128.
[42] J. Qian, W. Sun, Q. Zhang, G. Jiang, W. Liu, Fabrication and performance of BaCe0.8Y0.2O3-δ-BaZr0.8Y0.2O3-δ bilayer electrolyte for anode-supported solid oxide fuel cells, J. Power Sources 249 (2014) 131–136.
[43] L.S. Wang, C.X. Li, C.J. Li, G.J. Yang, Performance of La0.8Sr0.2Ga0.8Mg0.2O3-based SOFCs with atmospheric plasma sprayed La-doped CeO2 buffer layer, Electrochim. Acta 275 (2018) 208–217.
[44] D. Panuh, A. Muchtar, N. Muhamad, E.H. Majlan, W.R.W. Daud, Fabrication of thin Ag-YSB composite cathode film for intermediate- temperature solid oxide fuel cells, Compos. B Eng. 58 (2014) 193–198.
[45] A. Bodén, J. Di, C. Lagergren, G. Lindbergh, C.Y. Wang, Conductivity of SDC and (Li/Na)2CO3 composite electrolytes in reducing and oxidising atmospheres, J. Power Sources 172 (2007) 520–529.
[46] R. Sažinas, K.B. Andersen, S.B. Simonsen, P. Holtappels, K.K. Hansen, Silver modified cathodes for solid oxide fuel cells, J. Electrochem. Soc. 166 (2019) F79–F88.
[47] R.D. Shannon, Revised effective ionic radii and systematic studies of interatomic distances in halides and chalcogenides, Acta Crystallogr. A 32 (1976) 751–767.
[48] W. Sun, N. Zhang, Y. Mao, K. Sun, Facile one-step fabrication of dual-pore anode for planar solid oxide fuel cell by the phase inversion, Electrochem. Commun. 22 (2012) 41–44.
[49] A. Pesaran, A. Jaiswal, E.D. Wachsman, Bilayer electrolytes for low temperature and intermediate temperature solid oxide fuel cells – a review, in: S. Skinner (Ed.), Energy Storage Convers. Mater., The Royal Society of Chemistry, 2019, pp. 1–41.
[50] E.D. Wachsman, P. Jayaweera, N. Jiang, D.M. Lowe, B.G. Pound, Stable high conductivity ceria/bismuth oxide bilayered electrolytes, J. Electrochem. Soc. 144 (1997) 233–236.
[51] D.W. Joh, J.H. Park, D. Kim, E.D. Wachsman, K.T. Lee, Functionally graded bismuth oxide/zirconia bilayer electrolytes for high-performance intermediate-temperature solid oxide fuel cells (IT-SOFCs), ACS Appl. Mater. Interfaces 9 (2017) 8443–8449.